Polish Society of Composite Materials
Polskie Towarzystwo Materiałów Kompozytowych

20: 3-4 (2020) 134-141

COMPOSITES THEORY AND PRACTICE
ISSN: 2084-6096
ISSN (online): 2299-128X

Michał Sałaciński[1]*, Paweł Orzechowski[1], Marek Chalimoniuk[1], Andrzej Leski[2]

[1] Airworthiness Division, Air Force Institute of Technology, ul. Księcia Bolesława 6, 01-494 Warszawa, Poland
[2] Łukasiewicz Research Network – Institute of Aviation, al. Krakowska 110/114, 02-256 Warszawa, Poland
**Corresponding author. E-mail: michal.salacinski@itwl.pl*

Received (Otrzymano) 4.11.2020

ANALYSIS OF BONDING LAYER QUALITY IN REPAIR PROCESS OF AIRCRAFT COMPOSITE STRUCTURE AFTER IMPACT DAMAGE

Aircraft composite structures made in autoclave prepreg technology are characterized by low porosity and high strength. Unfortunately, composite structures are susceptible to impact damage. Therefore in order to repair this type of structures, an advantageous method of structure restoration is the use of the two-step bonding method. This method relies on creating a composite patch cured in an autoclave and then bonding it into a previously prepared repair area in the repaired structure, created by removing the damaged layers. Thanks to this approach, the patch is produced in accordance with the production process of the repaired element and has similar properties including low porosity. A critical element of repair is the bonding layer between the patch and repaired structure. Difficulties in obtaining an appropriate consolidation pressure (compression) using a vacuum bag can cause local disbonding of the composite patch as well as porosity in the bonding layer. Porosity reduces the strength properties of the joint, and it also reduces its weather resistance, which may contribute to its gradual degradation. The article focuses on analysis of the influence of compression obtained by a vacuum bag on the porosity and thickness of the bonding layer. A professional line for the production of aircraft composites and a mobile system for composite repairs of aircraft structures were used to produce the samples. The computed tomography method was used to measure the porosity and thickness of the bonding layer.

Keywords: bonding, composite repair, impact damage, porosity, computed tomography

INTRODUCTION

Continuous fiber reinforced epoxy composites are materials characterized by excellent strength properties and the ability to form virtually any shape. For these reasons, polymer composites are widely used in various industries, including aviation, aerospace, and automotive. In addition to their advantages, composites have the disadvantage of low resistance to dynamically introduced concentrated loads – impact damage.

Typical damage of laminar structures is caused by impacts of various energies. Damage in the scientific sector is classified according to the impact energy and velocity of the impactor [1-5], as schematically shown in Figure 1.

In aviation technology damage is classified as hard to detect BVID barely visible impact damage) or detectable VID (visible impact damage).

BVID is hard to detect as it does not affect the surface geometry. The standard damage of this type is caused by low energy impacts up to 5.4 J with a 25.4 mm diameter semi-spherical impactor. In operation, such energies are characteristic of impacts from debris from the runway during take-off and impacts from small birds. During maintenance this type of damage can also occur. It can be caused by the impacts of tools such as small wrenches or screwdrivers [6]. Upon this definition and the results of a radiogram presented in [6], it can be assumed that this type of damage is characteristic of low energy impact damage (Fig. 1a).

Barely visible damage, which may not be found during HMV (heavy maintenance general visual inspections), is not visible to the unaided eye under normal light conditions from a distance of about 1.5 m. This sort of damage occurs when hitting up to approximately 135 J with a 25.4 mm diameter semi-spherical impactor. In operation, such energies are characteristic of impacts caused by foreign objects or fragments of the runway during take-off and landing. During maintenance such damage can also occur, caused by the fall of large tools such as large wrenches, a hammer or a pneumatic drill [6]. Considering this definition and the results of the radiogram presented in [6], it can be assumed that this type of damage is characteristic of medium energy low speed impact damage (Fig. 1b).

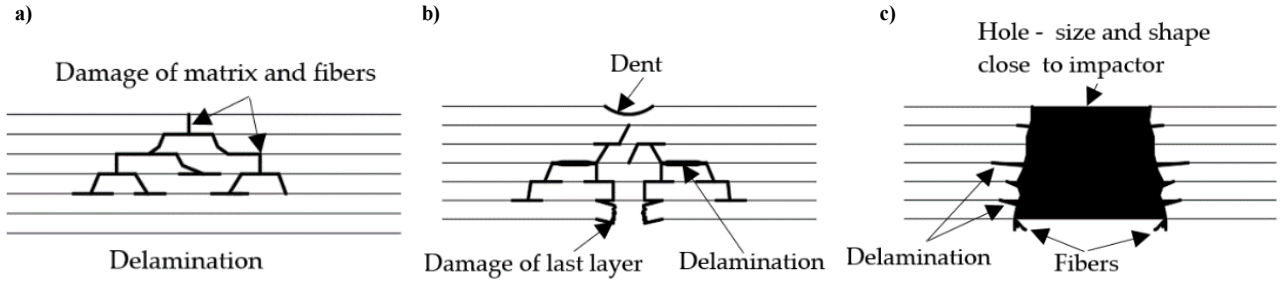

Fig. 1. Impact damage of epoxy-carbon composite (CFRP): a) low energy impact damage; b) medium energy, low speed impact damage; c) high energy, high speed impact damage

Visible impact damage (VID) above 135 J is damage detectable to the unaided eye under normal light conditions from a distance of about 1.5 m. Standard damage is also done with a 25.4 mm diameter semi-spherical impactor. In operation, such energies are primarily impacts of large birds or during collisions with other objects during taxiing. During maintenance, this type of damage is typically caused by accidental impacts of a hammer or other heavy tools. VID includes damage caused by high energy and high speed impacts (Fig. 1c). This damages concern mainly military aircraft and takes place during missions – also called battle damage [7], as shown in the example in Figure 2. This includes mainly bullet and shrapnel impacts.

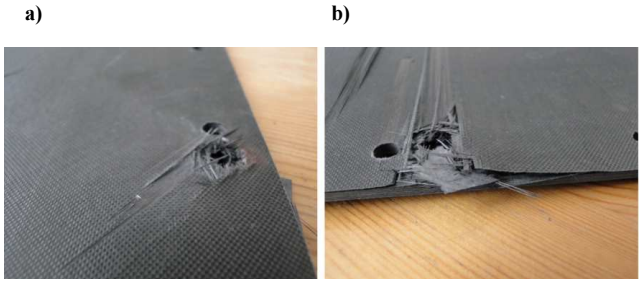

Fig. 2. Damage caused by high energy high speed impact: bullet hole (M4 carbine, caliber 5.56 mm) in specimen (40 layers unidirectional quasi-isotropic): a) entrance; b) exit

Each impact causes damage to the matrix and can cause damage to the fibers as well [2-5, 8]. These issues negatively influence the mechanical properties of the composite – they reduce its strength and stiffness. Therefore repair is necessary in order to return the structure to service.

Several different methods of repairing composite structure damage are used in aircraft maintenance. Most commonly, mechanical joints or adhesive bonding are used [9]. The methods using adhesive bonding are shown in Figure 3.

Structure strength properties. The structure can be restored during repair in several ways [10]: co-bonding, co-curing, secondary bonding and multi material bonding. The concept drawings of bonding are presented in Figure 4.

According to reference [11], a composite repaired with the scarf structure restoration method (Fig. 3a) and by means of secondary bonding (Fig. 4c) regains over 90% of its undamaged properties. This method is the most effective one used to date. The effectiveness of the method results from the fact that the composite patch is made in prepreg technology with the autoclave method and then the patch is bonded with the damaged structure using adhesive film. The autoclave method allows us to produce the composite patch in the same conditions as the original structure.

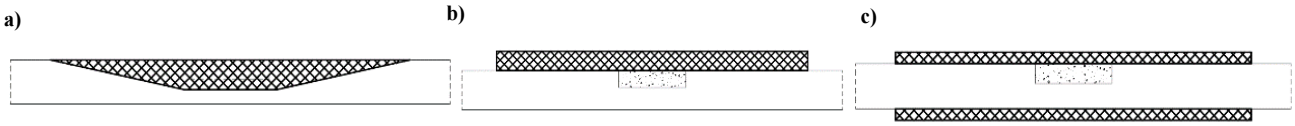

Fig. 3. Scheme of composite technology with adhesive bonding: a) scarf – restoration of structure; b) single-sided lap; c) double-sided lap

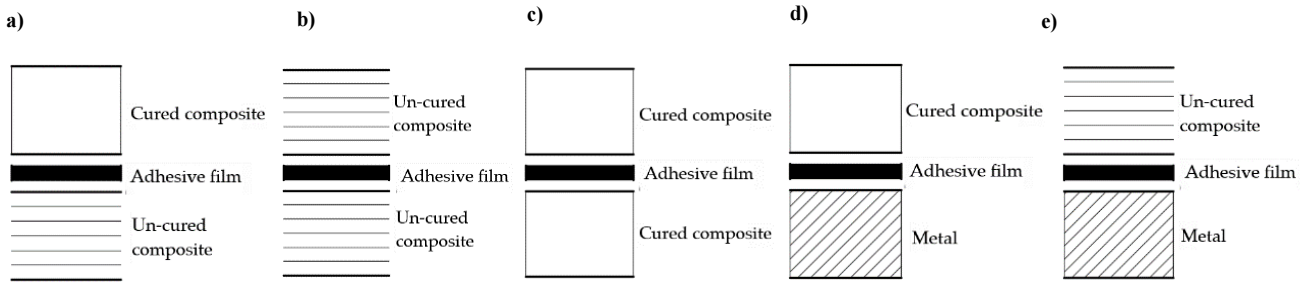

Fig. 4. Models of typical manufacturing bonding processes between composite components: a) co-bonding; b) co-curing; c) secondary bonding, d) and e) multi-material bonding

However, it should be borne in mind that repair effectiveness tests [11] were conducted on laboratory samples. In laboratory conditions, no problems with the assembly of the vacuum bag occur. Usually, the whole panel for samples is closed in a vacuum bag. Thus, the vacuum bag is always tight and the compression of the patch to the repair area caused by the bag reaches a maximum value of approximately 90 kPa. The vacuum in the bag is easily maintained for one minute after the vacuum pump is disconnected.

Unfortunately, an actual aircraft structure is more complicated. In a semi-shell structure, typical in modern aircraft, reinforcements in the form of girders, ribs, longerons and rebates are metal elements, to which composite sheathing is attached by means of mechanical connections. Damage to the composite structure often occurs on irregularly shaped surfaces, such as around rivets [12, 13] or at corners and edges. What is worse, it is precisely damage in these places that most threatens the structure [14].

A model of a fragment of a classical structure with damage is presented in Figure 5.

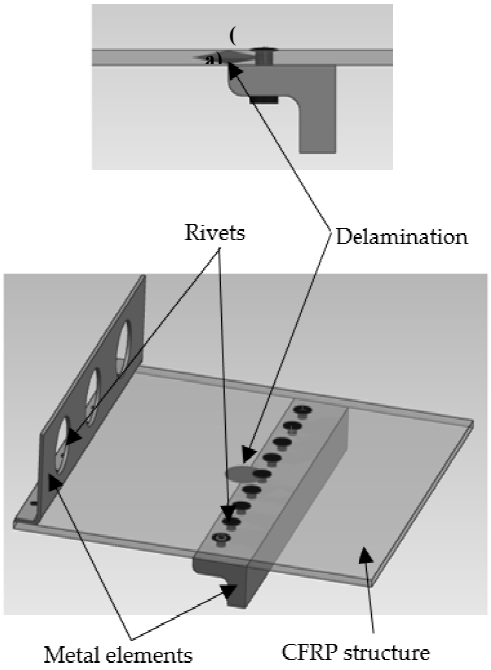

Fig. 5. Model of aircraft structure with impact damage delamination

The assembly and sealing of a vacuum bag on a large irregular surface is complicated, by rivets, overlapping joints or other openings, such as those presented in Figure 5, making this task much more complicated than for a simple laboratory sample. In addition, the resulting damage usually occurs across the entire cross-section of the structure, which requires a through-hole. Therefore, a problem occurs with sealing the hole from the other side of the repaired structure, which is inaccessible. A model of such repair is presented in Figure 6.

During repair of the actual structure, it is very difficult to achieve 90 kPa consolidation pressure in a vacuum bag with a low capacity mobile vacuum pump. It is even more difficult to fulfill the condition of holding a constant level of negative pressure in a vacuum bag after the pump is disconnected.

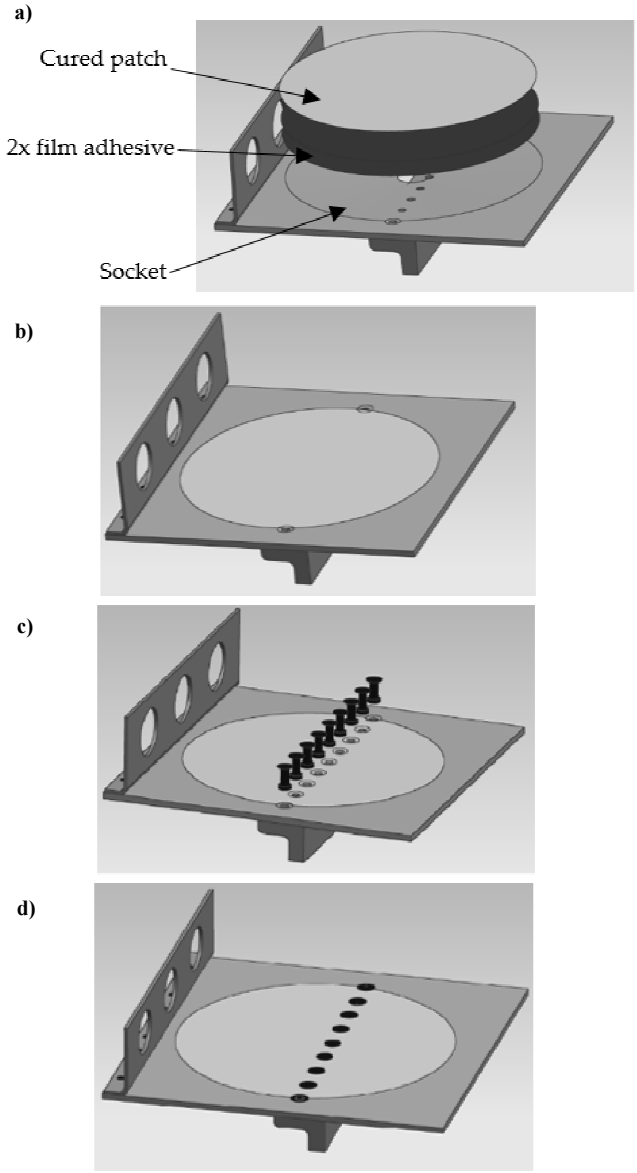

Fig. 6. Model of damage repair across section whole skin thickness: a) repair area and repair components, b) structure after curing adhesive films: c) riveting; d) structure after repair

MATERIALS AND EXPERIMENTAL PROCEDURE

The objective of our research was to find the impact of negative pressure and the tightness of the vacuum bag on the quality of the bond created using the secondary bonding method (Fig. 3c).

The thickness and the porosity of the bond after hardening between two composite panels was analyzed (Fig. 7).

The panels were created in the form of laminar composites with a quasi-isotropic structure $[(45/0/-45/90)_2/45/0]_s$. Each panel was composed of twenty 0.16 mm layers of E722-02 HS-14 12K 130g 35%rw

600 mm carbon epoxy UD prepreg material manufactured by TecCate. The curing cycle of the panel (Fig. 8) was conducted in an autoclave using aerospace technologies [1]. In total, eight panels were manufactured.

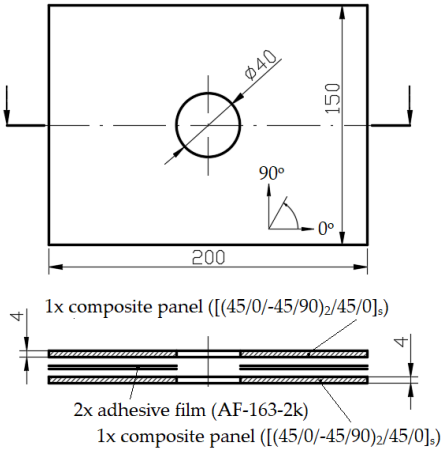

Fig. 7. Diagram of tested sample

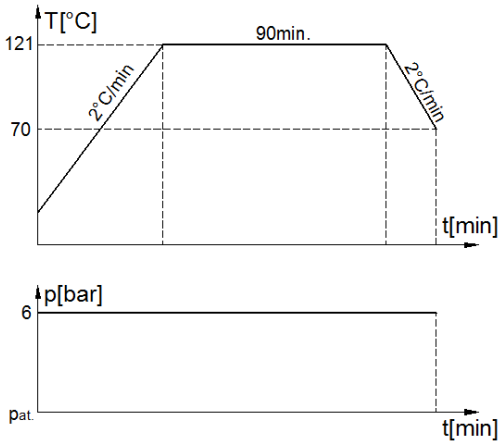

Fig. 8. Cure cycle of composite panels

The bond between the panels was made of two layers of 3M Scotch-Weld AF-163-2k (AF-163-2k) adhesive film. AF-163-2k adhesive film is commonly used in the aviation industry to bond metals and composites [15-17]. AF-163-2k adhesive film is stored at –18°C in its uncured condition. After unfreezing, the film is a flexible bonding layer. Flexibility and integrity are ensured by the resin applied to the polymer mesh (Fig. 9).

The first reason for conducting the research in this article is the discrepancy in information on the value of the negative pressure during bond hardening when AF-163-2k film is used. According to the technology sheet [18], AF-163-2 can be successfully cured by vacuum bag. To obtain the appropriate properties of the adhesive, the AF-63-2k adhesive film should be cured at a compressive pressure value of 27÷40 kPa (–0.27÷÷–0.4 bar). Moreover the technical datasheet [18] informs that higher compressive pressure values (lower pressure in the bag) can cause increased porosity and reduced joint strength. However, experience shows that this compressive pressure value is not sufficient for proper patch consolidation in a repair area. According to publications [1, 15, 19, 20], the compressive pressure value should be close to the maximum attainable with a vacuum bag. In practice, the vacuum bag allows us to attain a compressive pressure value at the level of 90 kPa (–0.9 bar).

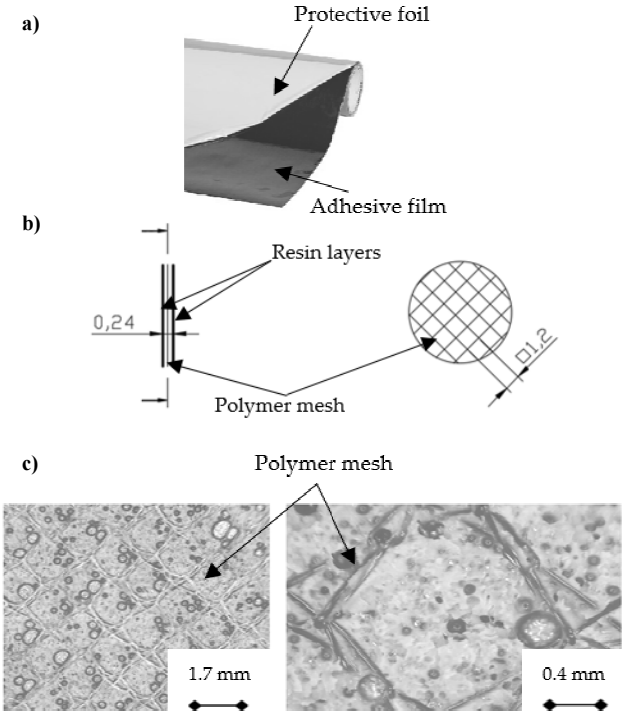

Fig. 9. 3M AF-163-2k adhesive film: a) uncured view; b) film construction; c) view of film after separation of adherent elements

The second reason for conducting the research in this article was to verify to what degree a leak or puncture of the vacuum bag impacts the quality of the bond.

In relation to the above, bond samples between panels hardened in vacuum bags were created at various compressive pressure values for further research:

- 30h – sample cured with a compressive pressure value of 30 kPa (–0.3 bar) in a sealed bag;
- 60h – sample cured with a compressive pressure value of 60 kPa (–0.6 bar) in a sealed bag;
- 90h – sample cured with a compressive pressure value of 90 kPa (–0.9 bar) in a sealed bag;
- 60l – sample cured with a compressive pressure value of 60 kPa (–0.6 bar) in a leaky bag.

While creating the 30h, 60h and 90h samples, the airtightness of the vacuum bag was verified and a reductor was used to set the compressive pressure value to 30 kPa (–0.3 bar), 60 kPa (–0.6 bar) and 90 kPa (–0.9 bar), respectively. The curing cycle was then launched.

While creating the 60l sample, the airtightness of the vacuum bag was also verified, and the compressive pressure value was set to 90 kPa (–0.9 bar) with the reductor. A needle was then used to create holes in the vacuum bag, in order to attain a compressive pressure

value of 60 kPa (–0.6 bar). After verifying that the compressive pressure value was stable, the curing cycle was launched.

The curing cycle was conducted using an electronically controlled heating blanket and following the heat curve presented in Figure 10.

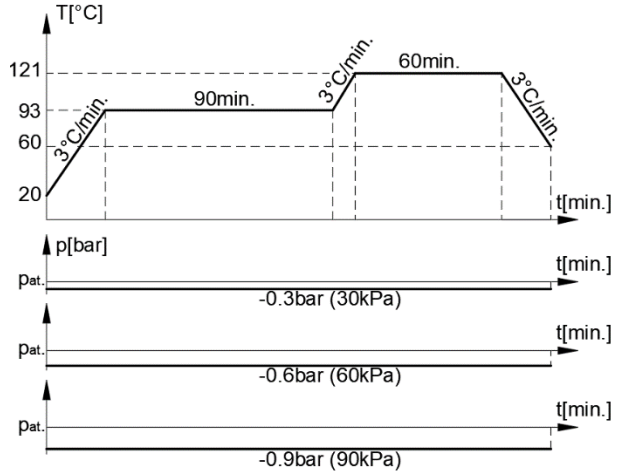

Fig. 10. Cure cycles of composite adhesive film

After the curing cycle of the adhesive film, a ϕ25 mm fragment was cut out of each sample for computed tomography testing, as shown in Figure 11.

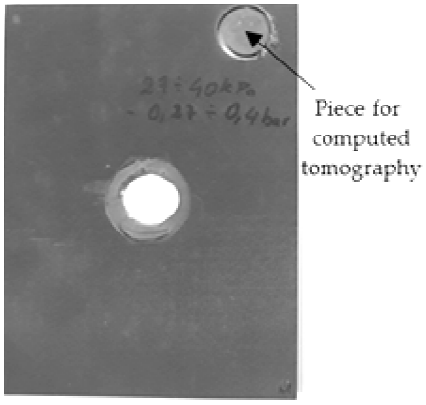

Fig. 11. Example sample after curing with leakage of adhesive film cured around hole

COMPUTED TOMOGRAPHY

Computed tomography (CT) was used to analyze the thickness and porosity of the bonding layer.

CT is a type of X-ray spectroscopy allowing tomographic images (cross-sections) of the examined object to be obtained, and then to present its spatial image (3D) from many plane view (2D) shots taken in different positions. CT modifies the scale of observation from macroscopic to microscopic which enables reliable results to be obtained [21]. Any difference in the material inside the object, a change in its density or voids can be visualized and measured. The examination consists in directing an X-ray beam to the object under examination and registering its intensity on the other side of the detector. Specialized software and computers with high computing power are used for the examination [22]. The discretization of the volume of the examined object is carried out by dividing it into single spatial cells called voxels (resolution). In each voxel the degree of absorbed radiation is constant.

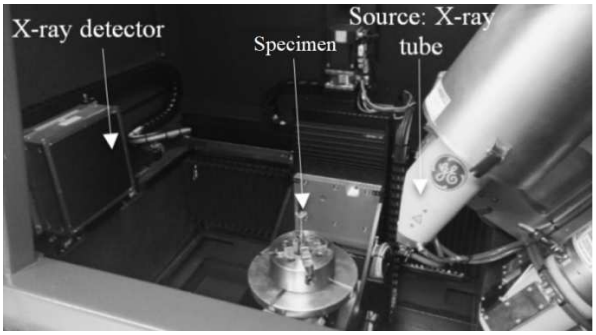

Fig. 12. Tomographic examination with panel detector – chamber of TC device during examination

X-radiation as well as other ranges of the electromagnetic spectrum can be absorbed and scattered by matter [23]. As a result of these processes, the radiation beam is weakened, which is a function of the radiation energy, type and thickness of the tested material. The change in radiation intensity of a parallel radiation beam of equal energy when passing through an object is described by relation (1):

$$I = I_0 \cdot e^{-\mu \cdot g} \tag{1}$$

where: I – radiation intensity after passing through the object [W/m^2], I_0 – initial radiation intensity [W/m^2], μ – linear coefficient of attenuation (absorption) of X-radiation characteristic of a given material and a specific wavelength [1/cm], g – thickness of the tested material [cm].

The advantage of the CT method is the three-dimensional image of the structure, and thus the ability to read the results relatively quickly and easily. CT shows the size, shape and location of voids as well as material contaminations and other heterogeneities [24]. The problem of using tomography is the limitations associated with the tomography chamber and the wall thickness of the element being examined – their overall size is important for the test. The required safe thickness of the cabin walls, constituting the radiation absorbing screen, increases with the increase in power and voltage of the devices [25].

The specimens were tested using a 300 kV lamp on a GE Phoenix v/tome/x m CT with a panel detector (Fig. 12). The tests were carried out with the following parameters:

- voltage 100 kV;
- current 100 mA;
- timing 333 ms.

A voxel size of 46 μm was obtained. 720 pictures were taken per full turn. The images were reconstructed on a graphic station using the Datos/x 2 program.

RESULTS AND DISCUSSION

The thickness of the bonding layer was measured on the pieces cut from the sample (Fig. 11). The thickness of the boding layer was tested by CT (Fig. 13).

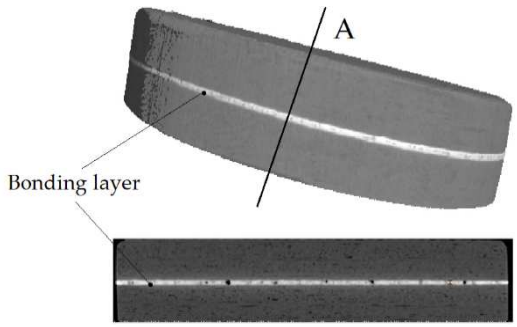

Fig. 13. Example of results of specimen (60h) tomography test, side view and cross section in plane A

The thickness of the bonding layer was measured in the VG Studio MAX 3.0 program with the "Caliper" measuring function. Six measurements were made for each specimen at various randomly selected locations. Next, the arithmetic average and standard deviation for individual specimens were calculated (Table 1).

TABLE 1. **Thickness of bonding layers**

Description	30h	60h	90h	60l
Values measured at six points for each sample/ specimen [mm]	0.27	0.21	0.18	0.23
	0.24	0.20	0.18	0.22
	0.24	0.20	0.19	0.21
	0.34	0.18	0.19	0.19
	0.24	0.19	0.19	0.18
	0.23	0.19	0.17	0.19
Arithmetic average [mm]	0.26	0.19	0.18	0.20
Standard deviation [mm]	0.04	0.01	0.01	0.02

In order to facilitate comparison of the bonding layer thickness, a diagram (Fig. 14) was made on the basis of the measurement results and calculations (Table 1).

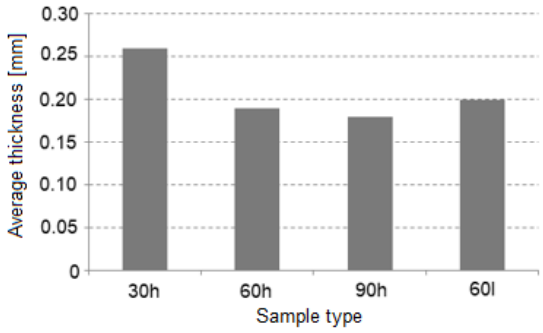

Fig. 14. Thickness of bonding layers

On the basis of the test results (Table 1 and Fig. 14), it can be concluded that the thickness of the bonding layer is dependent on the compressive pressure value. The thickness of the bonding layer is significantly higher when cured at the lower compressive pressure value of 30 kPa. At a higher compressive pressure value, although the difference in compressive pressure value is also 30 kPa, the difference in thickness is small. It should also be noted that at lower compressive pressure values the bonding layer is less even – the standard deviation is 0.04 mm.

The lack of tightness of the vacuum bag has practically no effect on the thickness of the bonding layer.

The percentage of porosity was determined by CT as well (Fig. 15), using the previously described phenomenon of radiation absorption by a higher density medium.

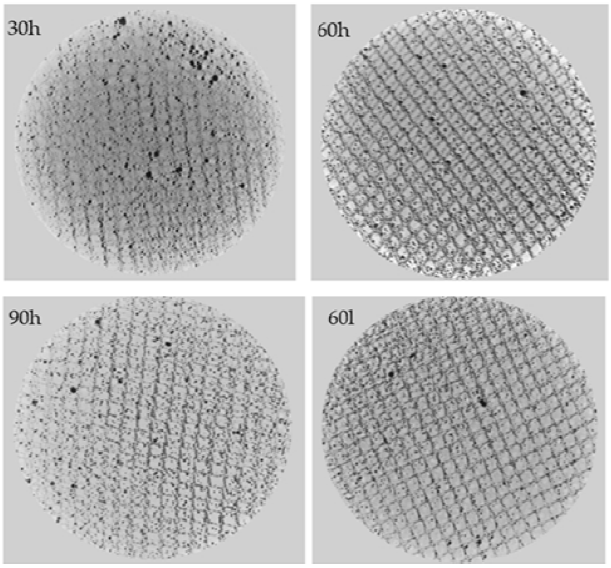

Fig. 15. Tomograms of bonding layers – cross-section made in plane parallel to glued layers in middle of bonding layer thickness

Porosity ξ is defined as the percentage share of the voids volume relative to the cured resin (2).

$$\xi = \frac{V_{voids}}{V_{bond}} \cdot 100\% \tag{2}$$

V_{voids} – volume of voids in the bonding layer, V_{bond} – monolithic cured resin volume in the bonding layer.

To analyze the porosity, VG Studio MAX 3.0 software was used. The results of the analysis are presented in Table 2.

TABLE 2. **Porosity level in bonding layer**

Mark	30h	60h	90h	60l
ξ [%]	1.33	0.39	1.56	0.59

In order to facilitate comparison of the porosity level of the bonding layer, a graph (Fig. 16) was made on the basis of the analysis results (Table 2).

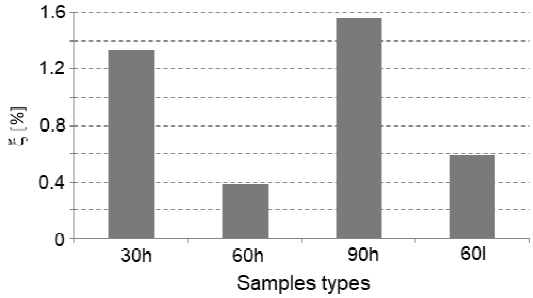

Fig. 16. Porosity level in bonding layer

Based on the results of the tests (Table 2 and Fig. 16), it can be concluded that the porosity level of the bonding layers depends on the compressive pressure value.

The above tests show that the porosity at the compressive pressure value induced by vacuum of –0.9 bar is higher than at the recommended –0.3 bar. Taking into account the results of the whole test, it can be assumed that the porosities of the 30h and 90h samples are at a similar level and are at an order of magnitude higher than the porosity of the 60h samples.

The porosity of samples 60h and 60l are on the same level.

CONCLUSIONS

The research aim was achieved. The conducted tests allowed us to demonstrate the influence of the compression caused by vacuum inside the bag on the quality of the bonding layers. The influence of the compressive pressure value on the thickness and porosity of the bonding layers was analyzed.

The studies show that the bonding layer thickness asymptotically decreases with the increase in vacuum in the bag.

A surprising phenomenon of the appearance of high porosity in the bonding layer at a high compressive pressure value in the vacuum bag was observed. One of the theories that can explain this phenomenon is cavitation of the components of the uncured bonding layer. The results of the research indicate that above a certain value of compressive pressure in the bag, some components of the uncured bonding layer start to evaporate. Therefore, in future, research will be continued to confirm this hypothesis.

The last important and beneficial conclusion from the point of view of the repair process is the proof that if adequate pressure is provided, leakage of the vacuum bag does not significantly affect the level of porosity of the bonding layer.

REFERENCES

[1] Advanced Composite Structures: Fabrication and Damage Repair, Teaching Materials, Abaris Training Resources. Reno NV, 2010.

[2] Szymański R., Non-destructive testing of the thermoplastic carbon composite structures, Transactions on Aerospace Research 2020, 1(258), 34-52, DOI: 10.2478/tar-2020-0003.

[3] Bona A., Theoretical and experimental review of applied mechanical tests for carbon composites with thermoplastic polymer matrix, Transactions on Aerospace Research 2019, 4(257), 55-65, DOI: 10.2478/tar-2019-002.

[4] Bajurko P., Wyznaczanie otworu ekwiwalentnego dla uszkodzeń poudarowych na podstawie badań wytrzymałości resztkowej (Determination of open hole equivalent to after impact damage based on residual strength tests), Prace Instytutu Lotnictwa 2016, 3(244), 20-27, DOI: 10.5604/05096669.1222731.

[5] Bobrowska M., Barcikowski M., Ocena uszkodzeń udarowych rur kompozytowych wykonanych metodą nawijania i zaprojektowanych według metody tablicowej (Assessment of impact damage to composite pipes made with the winding method and designed according to the table method), Prace Instytutu Lotnictwa 2016, 3(244), 26-40, DOI: 10.5604/05096669.1222734.

[6] Fawcett A.J., Oakes G.D., Boeing composite airframe damage tolerance and service experience, Boeing Commercial Airplanes, downloaded from the portal https://www.wichita.edu/.

[7] Leski A., Analiza wytrzymałości łopaty śmigłowca uszkodzonej w wyniku przestrzelenia (Strength analysis of damaged helicopter blade as a result of overshot), PhD thesis, Military University of Technology, Warsaw 2000.

[8] Ancelotti J.A.C., Use of the marlin criteria to determine the influence of porosity on the Iosipescu and short beam shear properties in carbon fiber polymer matrix composites, Materials Research 2010, 13, DOI: 10.1590/S1516-14392010000100014.

[9] Ahn S.H., Springer G.S,. Repair of composite laminates, U.S. Department of Transportation Federal Aviation Administration, Washington 2000, http://www.tc.faa.gov/its/worldpac/techrpt/ar00-46.pdf.

[10] Budhe S., Banea M., de Barros S.S., An updated review of adhesively bonded joints in composite materials, International Journal of Adhesion and Adhesives 2017, 72, DOI: 10.1016/j.ijadhadh.2016.10.010.

[11] Ushakov A., Probabilistic design of damage tolerant composite aircraft structures, U.S. Department of Transportation Federal Aviation Administration, Washington 2002, http://www.tc.faa.gov/its/worldpac/techrpt/ar01-55.pdf.

[12] Dragan K., Klimaszewski S., Nowoczesne metody badań nieniszczących (Modern methods of non-destructive testing), [In:] J. Lewitowicz, Problemy eksploatacji statków powietrznych (Problems of aircraft maintenance), Vol. 6, ITWL, Warszawa 2006.

[13] Puchała K., The influence of selected local phenomena in CFRP laminate on global characteristics of bolted joints, Materials, MDPI AG, 2019, 12, 4139, DOI: 10.3390/ma12244139.

[14] Kubiak T., Gliszczynski A., Krygier M., Impact damage tolerance of laminate short columns subjected to uniform compression – experimental investigation, Composite Structures 2019, 226/111222, DOI: 10.1016/j.compstruct.2019.111222.

[15] Baker A.A., Rose L.R., Advances in the Bonded Composite Repair of Metallic Aircraft Structure, Elsevier Science Ltd., Amsterdam, Boston, London, New York 2002.

[16] Baker A.A., Jones R., Bonded repair of aircraft structures, Martinus Nijhoff Publisher, Dorrdrecht 1988.

[17] Zabłocka M., The effect of cure cycle time on the properties of epoxy-bonded joints, Fatigue of Aircraft Structures 2013, 151-167, DOI: 10.2478/v10164-012-0066-1.

[18] Aerospace and Aircraft Maintenance Department. Scotch-Weld Structural Adhesive Film AF 163-2, Technical Datasheet 2009, www.3M.com/aerospace.

[19] Sałaciński M., Synaszko P., Olesiński D., Approach to evaluation of delamination on the MiG-29's vertical stabilizers composite skin, [In:] A. Niepokólczycki, J. Komorowski, ICAF 2019 – Structural Integrity in the Age of Additive Manufacturing, Springer Link, Krakow 2020, 865-873, https://link.springer.com/chapter/10.1007/978-3-030-21503-3_69.

[20] Szymczyk E., Influence of metal foil on interface stress state in CFRP laminate, Solid State Phenomena 2016, 223--231, DOI: 10.4028/www.scientific.net/SSP.250.223.

[21] Antolovich S.D., Bathias C., Bayraktar E., New developments in non-destructive controls, Journal of Materials Processing Technology 2008, DOI: 10.1016/j.jmatprotec. 2007.12.001.

[22] Spearing S.M., Three-dimensional assessment of low velocity impact damage in particle toughened composite laminates using micro-focus X-ray computed tomography and synchrotron radiation laminography, Composites Part A: Applied Science and Manufacturing 2013, DOI: 10.1016/j.compositesa.2013.05.003.

[23] Cygański A., Metody spektroskopowe w chemii analitycznej (Spectroscopic methods in analytical chemistry), Wydawnictwo Naukowe PWN Warszawa 1997.

[24] Vaara P., Leinonen J., Technology survey on NDT of carbon-fiber composites, Publications of Kemi-Tornio University of Applied Sciences 2012.

[25] Ratajczyk E., Tomografia komputerowa CT w zastosowaniach przemysłowych, Cz. II. Tomografy i ich parametry, przykłady zastosowań (CT computed tomography in industrial applications. Th. II. Tomographs and their parameters, examples of applications), Mechanik 2011, 84, 3, 226-228, http://www.mechanik.media.pl/.

